Journal of Engineering Physics and Thermophysics, Vol. 71, No. 5, 1998

PULSERS WITH A VARIABLE GEOMETRY OF THE WORKING VOLUME AND THE EFFECT OF PROCESSED COMPOSITES ON THE DYNAMIC CHARACTERISTICS OF PULSERS

A. I. Nakorchevskii, B. I. Basok, and
A. I. Chaika

UDC 532.54

We present a mathematical model of the operation of pulsers with flexible membranes that produce effects typical of hydraulic shocks. Such devices are used as effective extractors, dispersers, and emulsifiers. We show that the dynamic behavior depends on the physical properties and the composition of the medium being processed.

Facilities with a variable geometry of the working volume, shown in the schematic diagram in Fig. 1, have proved to be effective emulsifiers, dispersers, and extractors. They consist of chamber 1 with symmetrically positioned rubber membranes 2 and a connecting channel 3, whose lower part is immersed in the processed liquid medium 4. The side surfaces of the chamber are connected, by means of branch pipes 5, with high- (R) and low- (W) pressure gas vessels. The operating cycle of the facility is divided into two subcycles of successive connection of the chamber to the vessels R and W; it leads to displacement of the membranes to the middle position and the side surfaces of the chamber, respectively. This causes oscillatory motion of the processed medium in a continuous-flow loop, which is accompanied by dynamic phenomena of hydraulic-shock type.

The parameters of the flow in the connecting channel are determined by the theorem on the change in momentum in the form of a Lagrange-Cauchy integral, which in a one-dimensional approximation with account for energy losses has the form

$$\rho S_x I \frac{dv_x}{dt} + \left(\rho g Z + p + \rho \frac{v^2}{2}\right)_a + \rho (\Sigma\zeta) \frac{v_x^2}{2} \operatorname{sign}(v_x) = \left(\rho g Z + p + \rho \frac{v^2}{2}\right)_b, \tag{1}$$

where the quantity I denotes the geometric combination

$$I = \int_{x_b}^{x_a} \frac{dx}{S}; \tag{2}$$

the subscripts a and b in (1) relate the quantities to the cross sections x_a and x_b; the subscript x indicates the need to obey the correspondence between v and S according to the continuity equation. The sign of the quantity v_x corresponds to the direction of the x axis in Fig. 1. Expressions (1) and (2) acquire an especially simple form when S = const. After the rubber membranes have been pressed to the inner surfaces of the chamber, the elasticity of the rubber will result in the inflow of an additional amount of mixture in the time δt according to the equation

$$v_x S_x \delta t = \delta V_r = V_r \frac{\delta p_a}{E}, \tag{3}$$

which is valid in the region of elastic deformation of the rubber, or in differential form

Institute of Technical Thermophysics, National Academy of Sciences of Ukraine, Kiev. Translated from Inzhenerno-Fizicheskii Zhurnal, Vol. 71, No. 5, pp. 775-783, September-October, 1998. Original article submitted February 27, 1997.

1062-0125/98/7105-0757$20.00

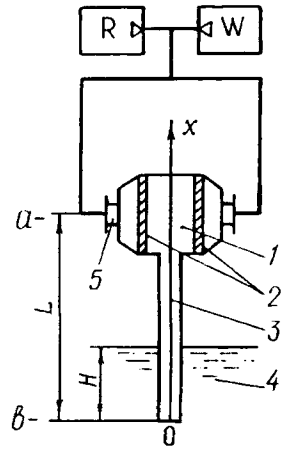

Fig. 1. Schematic of a pulser.

$$\frac{dp_a}{dt} = \frac{E}{V_r} S_x v_x . \tag{4}$$

In the case of outflow ($v_x < 0$), the pressure p_a will decrease according to Eq. (4).

In [1] the following assumptions were made: a) the rubber membranes are absolutely flexible and do not respond to tension forces; then the pressures on both sides of a membrane are identical; b) the gas routes do not offer substantial resistance to the motion of gas in them. Thus, when the chamber was connected both with the vessel R and with W, the pressure p_a was assumed to be equal to p_R or p_W, respectively, and the solution of Eq. (1) uniquely determined the functions $v_{xi} = v_{xi}(t)$ when the chamber was being filled (i = W) and emptied (i = R). The calculated time of these subcycles was determined by the integral

$$V_{ch} = \int_0^{t_i} |v_{xi}| \, S_x \, dt . \tag{5}$$

The system of equations (1), (4) made it possible to calculate shock phenomena and the damping vibrational process.

The practice of operating individual types of such facilities caused one to abandon the assumptions made in [1] because of the substantial resistance of the distributing gas-charging valves installed in them. If we assume that the gas escapes adiabatically through the valves, then the expressions for the mass flow rate of the gas G will have the form:

a) when connected to the vessel R:

$$G_R = -\mu_R f_R \sqrt{\left(\frac{2k}{k-1}\rho_R p_R\right)} \beta_R^{1/k} \sqrt{\left(1 - \beta_R^{\frac{k-1}{k}}\right)} ; \tag{6}$$

b) when connected to the vessel W:

$$G_W = \mu_W f_W \sqrt{\left(\frac{2k}{k-1}\rho_m p_m\right)} \beta_W^{1/k} \sqrt{\left(1 - \beta_W^{\frac{k-1}{k}}\right)} ; \tag{7}$$

here

$$\beta_R = \max\left[\frac{p_m}{p_R}, \left(\frac{2}{k+1}\right)^{\frac{k}{k-1}}\right], \quad \beta_W = \max\left[\frac{p_W}{p_m}, \left(\frac{2}{k+1}\right)^{\frac{k}{k-1}}\right]. \tag{8}$$

In calculating the volume flow rates of the gas Q_R and Q_W we can assume that the gas obeys the Clapeyron equation:

$$\rho_{mem} = \frac{p_{mem}}{RT_{ch}}. \tag{9}$$

The sagging of a membrane is determined by the pressure differential on it [2] and, consequently, there is a relationship between the volume displaced by the membrane and the pressures p_a and p_{mem}:

$$p_a = p_{mem} - A\frac{Eh}{R_{mem}^{10}}V^3, \tag{10}$$

where

$$V = -V_- + 0.5\int_0^t |v_x|\, S_x\, dt \tag{11}$$

on connection to the vessel R and

$$V = V_+ - 0.5\int_0^t v_x S_x dt \tag{12}$$

on connection to the vessel W. Calculations according to [2] give the value of the coefficient A within the range 0.587–0.889. Equations (10)-(12) show that the relationship between p_a and p_{mem} changes radically in transition through the plane of zero membrane sagging.

Using Eq. (9) at T_{ch} = const, the mass conservation equation for the gas in the chamber is transformed into equations that determine the change in the gas pressure p_{mem}:

$$\frac{dp_{mem}}{dt} = (Q_R - 0.5\,|v_x|\,S_x)\frac{p_{mem}}{V_{memR}} \tag{13}$$

on connection of the chamber to the vessel R and

$$\frac{dp_{mem}}{dt} = (0.5v_xS_x - Q_W)\frac{p_{mem}}{V_{memW}} \tag{14}$$

on connection of the chamber to the vessel W. The volumes V_{memR} and V_{memW} are as follows:

$$V_{memR} = V_0 + 0.5\int_0^t |v_x|\, S_x dt, \quad V_{memW} = V_0 + V_- + V_+ - 0.5\int_0^t v_x S_x dt. \tag{15}$$

The relations presented here suffice to calculate the changes in the dynamic characteristics of the facility on its connection to the vessel R (relations (1), (5), (6), (8)-(11), (13), (15)) and to the vessel W (relations (1), (5), (7)-(10), (12), (14), (15)), as well as the oscillatory process connected with hydraulic shock (relations (1), (4)). For some facilities it is also necessary to take into account vibrational phenomena appearing after the limiting contact of the membranes in the middle of the chamber. Since in this case the membranes are in a limiting position, a subsequent decrease in the pressure in the chamber p_a relative to the working-gas pressure p_{mem} will not cause displacement of the membranes. Subsequently, opposite conditions appear, i.e., $p_a > p_{mem}$, which are realized in hundredths-thousandths of a second and, due to the time lag of the mechanical system of the membranes, will also not lead to a change in their position. The more so, that the action of p_a is restricted to a narrow annular region. Therefore, in the case of the limiting position of the membranes only the influence of elastic deformation of the membrane material on the displacement of the medium in the section $a-a$ (see Fig. 1) must be taken into account:

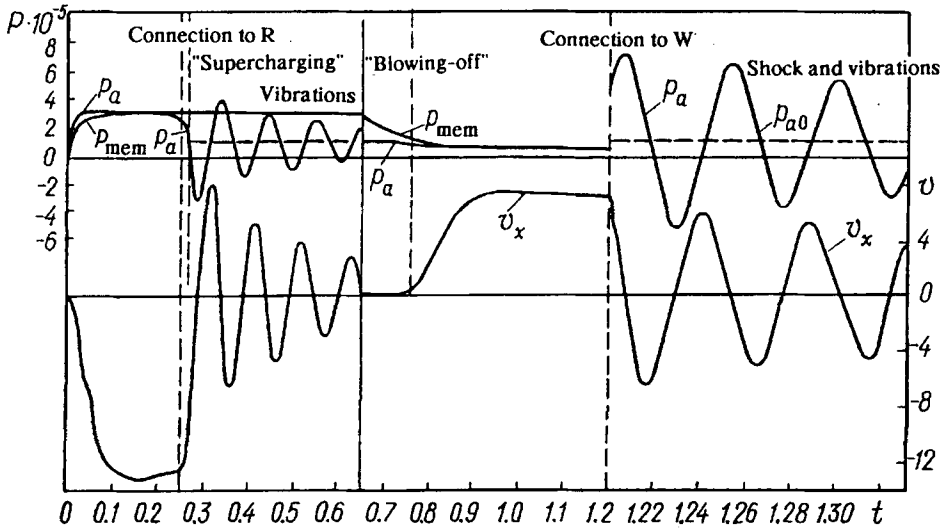

Fig. 2. Dynamic characteristics of a pulser in the case of a degassed liquid.

$$v_a = k_{\text{mem}} \frac{V_r}{S_x E} \frac{dp_a}{dt}, \tag{16}$$

where $k_{\text{mem}} \leq 1$. When the membranes are pressed to the side surfaces of the chamber, $k_{\text{mem}} = 1$. An example of calculation of such a pulsating facility is presented in Fig. 2 ($L = 0.75$ m, $H = 0.30$ m, $d = 0.1$ m, $S_x = 0.785 \cdot 10^{-2}$ m^2 = const, $p_R = 3 \cdot 10^5$ Pa, $p_W = 0.3 \cdot 10^5$ Pa, $p_H = 10^5$ Pa; the net volume of the chamber is $V_{ch} = 20.56 \cdot 10^{-3}$ m^3, the volume of the rubber membranes is $V_r = 2.95 \cdot 10^{-3}$ m^3 and that of the gas route is $V_0 = 3.92 \cdot 10^{-3}$ m^3, the effective area of the gas valves is $\mu_R f_R = \mu_W f_W = 9.03 \cdot 10^{-4}$ m^2, the elastic modulus of the rubber is $E = 5 \cdot 10^6$ Pa, the medium is degassed water, the working gas is air, $T = 293$ K, $k_{\text{mem}} = 0.2$ and 1.0). The initial conditions for the subcycle "connection to R" were the conditions of complete damping of oscillations at the end of the subcycle "connection to W":

$$v_x(0) = 0, \quad p_a(0) = p_{a(0)}, \quad p_{\text{mem}}(0) = p_W, \tag{17}$$

and the initial conditions for the subcycle "connection to W" were

$$v_x(0) = 0, \quad p_a(0) = p_{a(0)}, \quad p_{\text{mem}}(0) = p_R, \tag{18}$$

where $p_a(0)$ is the hydrostatic pressure calculated from Eq. (1) for $v_x = dv_x/dt = 0$.

In Fig. 2 vibrational phenomena are represented by several periods. For the time being we will refrain from commenting on the data obtained. We will only emphasize that the processed medium was assumed to be degassed, entirely incompressible, and "rigid," and this led to the possibility of passage of pressures to the negative region of values.

At the same time there are a number of liquid systems that contain a certain amount of gas dissolved in them and/or tend toward vapor formation on pulsation treatment. Sometimes a technology of treatment leads to penetration of a certain amount of gas into the chamber. The vapor-gas phase in such systems already acts as a damping factor on the dynamics of the pulsating processes that develop in the chamber and the connecting channel. For a reliable description of these phenomena in the case of a "nonrigid" processed medium, the latter must already be considered as two-phase with possible interphase momentum, mass, and energy transfer. According to [3, 4], the system of equations of motion for a two-phase barotropic medium in the spatially one-dimensional approximation has the form

$$\frac{\partial}{\partial t}(\rho_i B_i S) + \frac{\partial}{\partial x}(\rho_i B_i v_i S) = (\dot{M}_{ji} - \dot{M}_{ij}) S, \tag{19}$$

$$\rho_i B_i S \frac{\partial v_i}{\partial t} + \rho_i B_i v_i S \frac{\partial v_i}{\partial x} = \rho_i B_i G_x S_x \frac{\partial Z}{\partial x} - B_i S \frac{\partial p}{\partial x} -$$

$$- B_i \tau_i 2\pi R_{\text{chan}} - \dot{M}_{ji} (k_{ji}^{(p)} v_j - v_i) S + (F_{ji,m} + F_{ji,f}) S ,$$

$$B_i + B_j = 1 \quad (i, j = 1, 2) .$$

Numerous calculations showed [4] that under nonuniform and unsteady-state conditions of motion the effect of the additional mass on the vapor-gas phase leads to a comparatively small relative "slippage" of the phases. Therefore, in a first approximation we assume

$$v_1 = v_2 = v , \tag{20}$$

which substantially simplifies the equation of the dynamics in system (19). Moreover, in view of the small mass content of the vapor-gas phase compared to the liquid phase the equation of the dynamics can be neglected for the gas-vapor phase. Then system (19) will have the form

$$\begin{gathered}
\frac{\partial}{\partial t} (\rho_1 B_1 S) + \frac{\partial}{\partial x} (\rho_1 B_1 v S) = (\dot{M}_{21} - \dot{M}_{12}) S , \\
\frac{\partial}{\partial t} (\rho_2 B_2 S) + \frac{\partial}{\partial x} (\rho_2 B_2 v S) = (\dot{M}_{12} - \dot{M}_{21}) S , \\
\rho_1 \frac{\partial v}{\partial t} + \rho_1 v \frac{\partial v}{\partial x} = \rho_1 G_x \frac{\partial Z}{\partial x} - \frac{\partial p}{\partial x} - \frac{\tau_1}{R} , \\
B_1 + B_2 = 1 .
\end{gathered} \tag{21}$$

Integrating Eqs. (21) over x from x_b to x_a (see Fig. 1), for the case S = const we have

$$\begin{gathered}
\int_{x_b}^{x_a} \frac{\partial B_1}{\partial t} dx + (B_1 v)_a - (B_1 v)_b = \int_{x_b}^{x_a} \frac{(\dot{M}_{21} - \dot{M}_{12})}{\rho_1} dx , \\
\int_{x_b}^{x_a} \frac{\partial (\rho_2 B_2)}{\partial t} dx + (\rho_2 B_2 v)_a - (\rho_2 B_2 v)_b = \int_{x_b}^{x_a} (\dot{M}_{12} - \dot{M}_{21}) dx , \\
\rho_1 \int_{x_b}^{x_a} \frac{\partial v}{\partial t} dx + \int_{x_b}^{x_a} \frac{\tau_1}{r} dx + \left(\rho_1 g Z + p + \rho_1 \frac{v^2}{2} \right)_a = \left(\rho_1 g Z + p + \rho_1 \frac{v^2}{2} \right)_b , \\
B_1 + B_2 = 1 ,
\end{gathered} \tag{22}$$

where r is the hydraulic radius of the channel.

Let us consider conditions that make it possible to determine more precisely the form of the functions entering into Eq. (22) and the values of some of them on the boundaries of the region of integration. To increase the efficiency of pulsation treatment of the medium the amount of the "expelled–absorbed" portion of it must be minimal, at least it must not exceed a tenth of the connecting channel volume. The pressure p_b in the section b–b is close to atmospheric, and the amount of the vapor-gas component in the mixture under such conditions is small. Therefore, we may assume that in pulsation treatment there is no change in the mass of the vapor-gas phase due to mixture motion in the connecting channel. The quantities entering into Eq. (22) are functions of x and t, and for multiperiod oscillations the solution of system (22) is rather laborous. System (22) can be simplified considerably with an accuracy sufficient for practice, if one is guided by to certain mean values of the quantities

over the channel length $L = (x_a - x_b)$. Using the mean-value theorem with account for the foregoing, Eqs. (22) are transformed to

$$L\frac{d\langle B_1\rangle}{dt} + (B_1 v)_a - (B_1 v)_b = L\frac{\langle \dot{M}_{21}\rangle - \langle \dot{M}_{12}\rangle}{\rho_1},$$

$$\frac{d(\langle \rho_2\rangle \langle B_2\rangle)}{dt} = \langle \dot{M}_{12}\rangle - \langle \dot{M}_{21}\rangle,$$

$$\rho_1 L\frac{d\langle v\rangle}{dt} + \rho_1(\Sigma\zeta)\frac{\langle v\rangle^2}{2}\operatorname{sign}\langle v\rangle + \left(\rho_1 g Z + p + \rho_1\frac{v^2}{2}\right)_a = \left(\rho_1 g Z + p + \rho_1\frac{v^2}{2}\right)_b, \tag{23}$$

$$\langle B_1\rangle + \langle B_2\rangle = 1.$$

The notation in angular brackets relates the quantities to the mean values over the channel length, $(\Sigma\zeta)$ is the overall coefficient of hydraulic resistances in the continuous-flow circuit. The value of v_a is calculated from Eq. (16). We consider that the parameters of the vapor-gas component are determined by the Clapeyron equation:

$$\langle p\rangle = \langle \rho_2\rangle RT_2. \tag{24}$$

In the case of adiabatic vapor generation, T_2 should be assumed to be equal to the saturation temperature, $T_2 = T_s(\langle p\rangle)$ [4]. The values of the quantities on the boundaries of the region of integration can be connected with their mean values by linear relations:

$$p_a \doteq 2\langle p\rangle - p_b, \quad v_b \doteq 2\langle v\rangle - v_a, \quad B_{1a} \doteq 2\langle B_1\rangle - B_{1b}, \tag{25}$$

where B_{1b}, p_b can be assumed to be constant and to be determined from the conditions at the cut of the connecting channel. It can also be assumed that the regime of motion in the channel is close to complete mixing. Then from the last two relations of (25) we have

$$v_b = \langle v\rangle, \quad B_{1a} = \langle B_1\rangle \quad \text{when} \quad \langle v\rangle \le 0;$$

$$v_b \doteq \frac{\langle v\rangle\langle B_1\rangle}{B_{1b}}, \quad B_{1a} = 1 \quad \text{when} \quad \langle v\rangle > 0. \tag{25a}$$

We assume that the vapor-gas phase in the connecting channel has the form of spherical bubbles and is characterized by their number N_2 and the representative radius $\langle R_2\rangle$. The latter can be found from the balance relation:

$$\langle R_2\rangle = \sqrt[3]{\left(\frac{3\langle B_2\rangle}{4\pi n_2}\right)}, \tag{26}$$

where $n_2 = N_2/LS$ is the number density of the bubbles. The volume density of the rate of interphase transfer is determined according to the Hertz–Knudsen–Langmuir formula:

$$\langle \dot{M}_{12}\rangle = \frac{2\beta_a}{2-\beta_a}\left(\frac{M}{2\pi R_\mu}\right)^{0.5}\left(\frac{p_s(T_1)}{T_1^{0.5}} - \frac{\langle p\rangle}{T_2^{0.5}}\right)\frac{3\langle \beta_2\rangle}{\langle R_2\rangle},$$

$$\langle \dot{M}_{21}\rangle = \frac{2\beta_a}{2-\beta_a}\left(\frac{M}{2\pi R_\mu}\right)^{0.5}\left(\frac{\langle p\rangle}{T_2^{0.5}} - \frac{p_s(T_1)}{T_1^{0.5}}\right)\frac{3\langle \beta_2\rangle}{\langle R_2\rangle}, \tag{27}$$

where the accommodation coefficient $\beta_a \le 0.8$. Thus, the system of equations (16), (23)-(27) consists of three ordinary differential equations of first order that enter into Eq. (23), which should be solved for $d\langle B_1\rangle/dt$, $d\langle p\rangle/dt$

(using Eq. (24)) and $d\langle v\rangle/dt$, and algebraic relations. The expenditure of thermal energy for vapor generation in the connecting channel is so small that it is admissible to assume the liquid-phase temperature to be $T_1 = \text{const}$. It can easily be verified that system (16), (23)-(27) turns out to be closed on introduction of the approximations $T_2 = T_s(\langle p\rangle)$, $p_s = p_s(T_1)$ and assignment of n_2 and the initial value R_{20} (or B_{20}).

Let us now consider the case where initially there is a certain quantity of gas in the chamber and the level of the "rigid" medium at the time $t = 0$ has the mark Z_0 reckoned from the lower cut of the channel. If we assume that the gas parameters obey Eq. (24) and the cross section of the channel is constant, then the computational system of equations will have the form

$$\frac{dv}{dt} = \frac{1}{\rho Z}\left(p_H + \rho g H - p_a - \rho g Z - (\Sigma\zeta)\rho\frac{v^2}{2}\operatorname{sign} v\right),$$

$$\frac{dZ}{dt} = v, \tag{28}$$

$$p_a = p_{a0}\frac{L - Z_0}{L - Z}.$$

Under the initial conditions

$$t = 0, \quad v = v_0, \quad Z = Z_0, \quad p_a = p_{a0} \tag{29}$$

we have a Cauchy problem. Here $\Sigma\zeta = 1 + \lambda Z/d$.

Thus, we have mathematical models that describe the dynamics of the processes in facilities with a variable volume in the cases: A – of a degassed ("rigid") processed medium (1)-(16); B – of a medium with gas inclusions, shock phenomena in which are described by Eqs. (16), (23)-(26) at $\dot{M}_{ji} = 0$ ($i, j = 1, 2$); C – of a medium with interphase transitions (evaporation–condensation), shock phenomena in which occur according to Eqs. (16), (23)-(27); D – of a medium with a gas cavity in the chamber according to the additional equations (28) and (29).

Model C is divided into two submodels: C1 (with the assumption of possibly complete vapor-phase condensation) and C2 (for the case of a binary gas having a noncondensing component (for example, a steam–air system)). It should be emphasized that here relations are given that describe vibrational phenomena after the pressing of the membranes against the side surfaces of the chamber or after the limiting contact of the membranes in the middle plane of the chamber. The subcycles "connection to R" (expulsion of the medium from the chamber) and "connection to W" (intake of the medium into the chamber) are common to all the models; they are interpreted according to the dependences given in the beginning of the paper.

To reveal the special features of each of the models enumerated above, we carried out numerical solutions of the corresponding systems of equations for a pulsating facility with the parameters given above, to which the initial conditions for the bubbles must be added: $n = 10^{10}$ m^{-3}, $R_{20} = 3.6\cdot10^{-5}$ m, $\beta_a = 0.04$. The thermophysical parameters of steam were calculated according to the approximations given in [4].

As has already been noted, Fig. 2 presents the dynamics of the changes in the pressures and velocities according to "rigid" model A. The duration of the subcycle "connection to the vessel R" itself was 0.26 sec and the speed of expulsion of the medium from the chamber exceeded 12 m/sec. After complete expulsion of the liquid from the chamber, due to the limiting rigidity of the medium (the elasticity modulus $E_{med} \to \infty$) instantaneous deceleration of it occurs, which is accompanied by a pressure drop in the chamber to the level determined by the hydrostatic conditions. Since at the instant of deceleration the pressure of the working gas on the membrane p_m was somewhat below the pressure p_R in the receiver R, "supercharging" of the gas to the value $p_{mem} = p_R$ occurs in about 0.01 sec. The equilibrium developed in this case in the system may persist indefinitely. After transition to the subcycle "connection to the vessel W" the conditions of hydrostatic equilibrium in the chamber and the connecting channel will be preserved until the working-gas pressure p_{mem} falls to the value p_a ("blowing-off of the gas"), followed by speeding-up of the liquid characterized by a drop in the pressure in the chamber p_a virtually to the value p_W and by attainment of an intake velocity on the order of 7 m/sec. After the pressing of the membranes

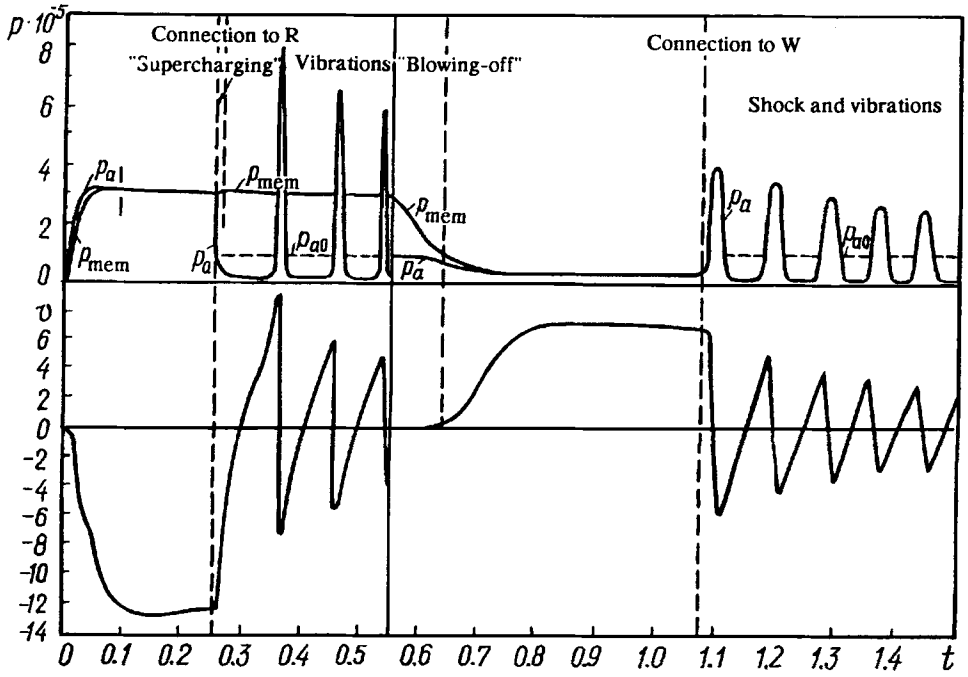

Fig. 3. Dynamic characteristics of a pulser in the case of a liquid with gas bubbles.

to the side surfaces of the chamber and deceleration of the medium, smoothed by the elasticity of the rubber diaphragms, a pressure increase and then a decrease in it occur with a corresponding change in the direction of medium motion. The amplitudes of the changes in the pressure and velocity attain values that exceed $6 \cdot 10^5$ Pa and 6 m/sec, respectively. The frequency of damped vibrations is $f_v \approx 20$ Hz. It is natural that the limiting rigidity of the medium was responsible for the transition of pressures to the region of negative values.

The dynamics of the vibrational processes will be quite different in the case of implementation of model B, presented in Fig. 3. Here, the medium processed was considered to contain air bubbles with a number density of inclusions $n_{20} = 10^{11}$ m^{-3}, an initial radius $R_{20} = 1.68 \cdot 10^{-5}$ m, and a constant temperature $T_2 = T_1 = 293$ K. Equation (24) does not allow one to cross the zero threshold of pressure values. A region of very low pressures decreasing to $0.001 \cdot 10^5$ Pa appears that is extended in time and subsequently converts into small zones of pulselike high pressures (up to $8 \cdot 10^5$ Pa). A comparison of the vibrational processes that followed the pressing of the membranes in the middle plane of the chamber (a time segment from $t = 0.25$ sec) and the pressing of the membranes to the side surfaces of the chamber (a time segment from $t = 1.085$ sec) shows distinctly the effect of the dynamic pressure of the medium at the instant of deceleration. The larger this pressure, the narrower the zones of pulsed pressures and the higher their greatest values.

Since, as noted above, the "speeding-up" subcycles are identical for all the models, Fig. 4 demonstrates the change in the fundamental parameters of the vibrational phenomena respectively after the pressing of the membranes in the middle plane of the chamber and after the pressing of the membranes to the side surfaces of the chamber for model C2. It was assumed that the noncondensing portion of the gas-vapor phase $M_{20} = 4.18 \cdot 10^{-3}$ kg and that the water temperature was increased to the value $T_1 = 383$ K. Calculations showed that a characteristic feature of vapor generation in model C is a very slight decrease in the pressure $\langle p \rangle$ with respect to the saturation pressure p_s. Therefore, the lower threshold of pressures here is substantially higher than the lower threshold obtained in calculations by model B.

The region of low pressures was also found to be more extended. A pronounced increase in the frequency of vibrations in the course of their damping was also established. The plot that characterizes the change in the function $\langle B_1 \rangle$ presents the time segments of the durations of vapor generation, condensation, and compression-expansion of the noncondensing portion of the gas-vapor phase, denoted by v.g., cond., and c.-e., respectively.

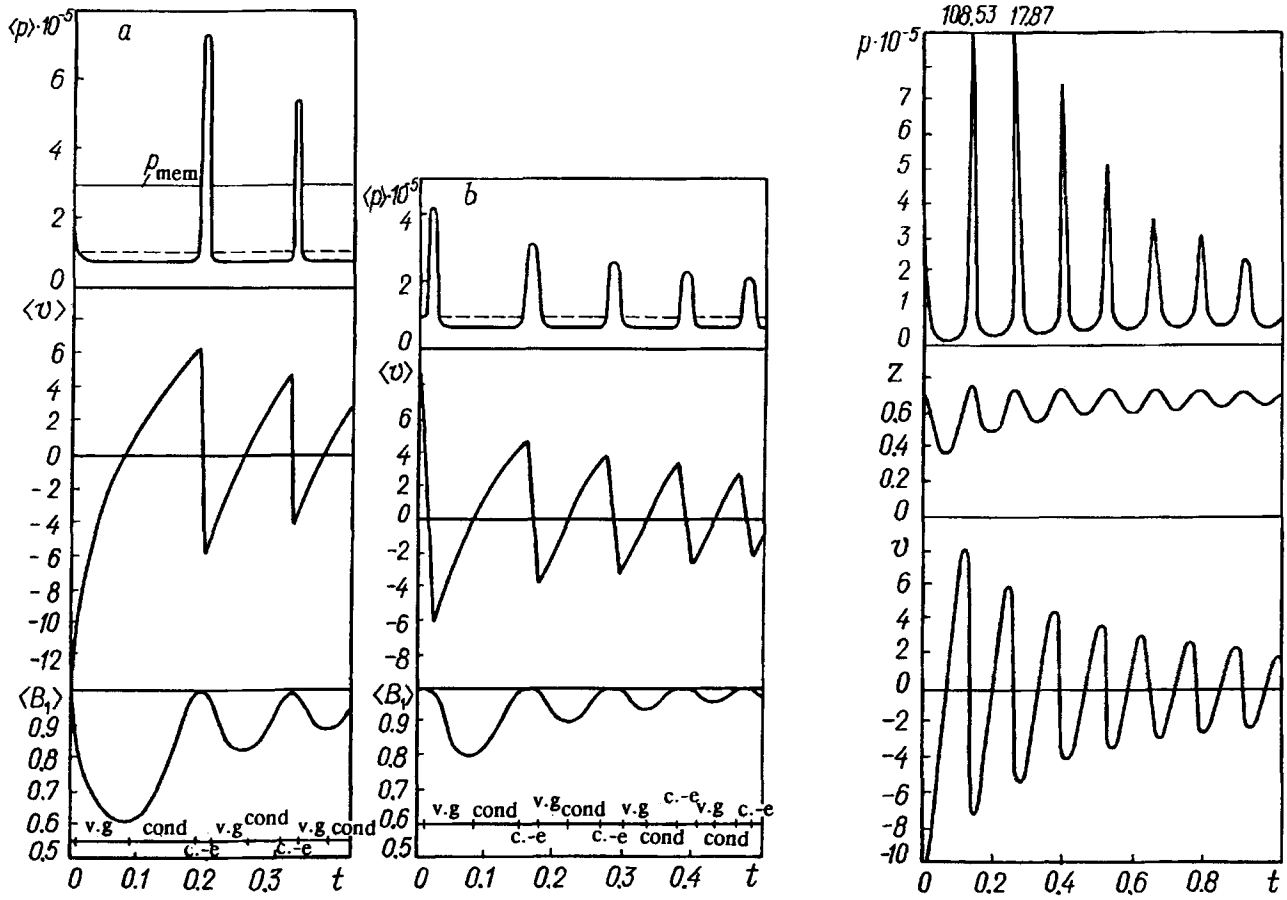

Fig. 4. Dynamic characteristics of a pulser in the case of a medium with interphase transitions (evaporation–condensation) after the pressing of the membranes in the middle plane of the chamber (a) and against its side surfaces (b).

Fig. 5. Dynamic characteristics of a pulser in the case of partial filling of the chamber with gas after the pressing of the membranes in the middle plane of the chamber.

Finally, Fig. 5 presents results of calculations by model D under the following initial conditions: $t = 0$, $v_0 = -12.52$ m/sec, $Z_0 = 0.73$ m, $p_{a0} = 2.89 \cdot 10^{-5}$ Pa. As follows from Fig. 5, the presence of a comparatively small gas cavity (of the height $h = L - Z_0 = 0.02$ m) confined to the upper portion of the facility leads to the development of highly intense dynamic effects. Here the calculated peak pressure attains values of the order of 10^7 Pa. True enough, the extreme values of the pressures damp very rapidly. With a decrease in the initial value Z_0, the damping effect of the gas increases (when $Z_0 = 0.72$ m, $p_{a\max} = 15 \cdot 10^5$ Pa; when $Z_0 = 0.70$ m, $p_{a\max} = 4.7 \cdot 10^5$ Pa).

It follows from the foregoing that comparatively simple methods of variation of the properties of the medium treated lead to substantially different dynamic parameters of pulsating devices. Therefore, the mathematical models presented here make it possible to compose the treated media intentionally in order to obtain the final result required.

NOTATION

d, channel diameter, m; H, depth of immersion of the connecting channel into the medium, m; L, length of the connecting channel, m; E, elasticity modulus of the rubber, N/m^2; F_m, F_f, volumetric density of the interphase-interaction force due to the additional mass and velocity nonequilibrium, respectively, N/m^3; f, open area of the valve, m^2; G_x, volumetric density of mass forces in the x direction, m/sec^2; $g = 9.81$ m/sec^2; h, thickness

of a membrane, m; Q, volumetric flow rate, m^3/sec; k, adiabatic exponent; $k^{(p)}$, efficiency of pulse transfer; M, mass of a kilomole, kg/kmole; $\dot{M}$, volumetric density of the rate of interphase mass transfer, $kg/(sec \cdot m^3)$; p, pressure, N/m^2; R_{mem}, radius of a membrane, m; R_{chan}, radius of the connecting channel, m; S, open area of the channel, m^2; T, temperature, K; T_s, saturation temperature, K; t, time, sec; V, volume between a membrane and the plane of its zero sagging, m^3; V_+, portion of the working volume of the chamber between the middle plane of the chamber and the plane of zero sagging, m^3; V_-, same between the side surface of the chamber and the plane of zero sagging, m^3; V_0, volume of the gas cavity between the valve and the chamber, m^3; V_r, volume of the rubber membranes, m^3; V_{ch}, working volume of the chamber, m^3; v, velocity, m/sec; x, longitudinal coordinate, m; Z, leveling height, m; R, gas constant, $J/(kg \cdot K)$; R_μ, universal gas constant, $J/(kmole \cdot K)$; B, indicator function of a phase; $\Sigma\zeta$, coefficients of hydraulic resistances; λ, coefficient of hydraulic friction; μ, coefficient of discharge of the valve; ρ, density, kg/m^3; τ, wall-friction stress, N/m^2. Subscripts: a, b, x, parameters in the cross sections a, b, x (see Fig. 1); ch, parameters in the chamber; mem, parameters of the gas acting on a membrane; med, medium; i, j, number of a phase; $i, j = 1$, the liquid phase; $i, j = 2$, the gas-vapor phase; ij, parameters of the transition $i \rightarrow j$ on the phase interface ij.

REFERENCES

1. A. A. Dolinskii, A. I. Nakorchevskii, and A. A. Korchinskii, Dokl. Akad. Nauk Ukrainy, No. 2, 89-94 (1994).
2. S. P. Timoshenko and S. Voinovskii-Kriger, Plates and Shells [in Russian], Moscow (1966).
3. A. I. Nakorchevskii, B. I. Basok, and I. V. Gaskevich, Teplofiz. Vysok. Temp., 29, No. 6, 1121-1126 (1991).
4. A. A. Dolinskii, B. I. Basok, S. I. Gulyi, A. I. Nakorchevskii, and Yu. A. Shurchkova, Discrete-Pulsed Introduction of Energy in Heat Technologies [Russian translation], Kiev (1996).